Published in final edited form as:
Pharm Res. 2008 December ; 25(12): 2910–2919. doi:10.1007/s11095-008-9683-3.

Synthesis and Evaluation of a Well-defined HPMA Copolymer-Dexamethasone Conjugate for Effective Treatment of Rheumatoid Arthritis

Xin-Ming Liu[1,4], **Ling-Dong Quan**[1,4], **Jun Tian**[1], **Yazen Alnouti**[1], **Kai Fu**[2], **Geoffrey M. Thiele**[3], and **Dong Wang**[1,5]

1*Department of Pharmaceutical Sciences, University of Nebraska Medical Center, Omaha, NE 68198, USA*

2*Department of Pathology and Microbiology, University of Nebraska Medical Center, Omaha, NE 68198, USA*

3*Department of Internal Medicineheumatology Division, University of Nebraska Medical Center, Omaha, NE 68198, USA*

Abstract

Purpose—To develop a pH-sensitive dexamethasone (Dex)-containing *N*-(2-hydroxypropyl) methacrylamide (HPMA) copolymer conjugate with well-defined structure for the improved treatment of rheumatoid arthritis (RA).

Methods—A new pH-sensitive Dex-containing monomer (MA-Gly-Gly-NHN=Dex) was synthesized and copolymerized with HPMA using reversible addition-fragmentation transfer (RAFT) polymerization. The structure of the resulting HPMA copolymer-Dex conjugate (P-Dex) was analyzed and its therapeutic efficacy was evaluated on adjuvant-induced arthritis (AIA) rats.

Results—P-Dex was synthesized with controllable molecular weight and polydispersity index (PDI). The Dex content can be controlled by the feed-in ratio of MA-Gly-Gly-NHN=Dex. The P-Dex used for *in vitro* and *in vivo* evaluation has a weight average molecular weight (M_w) of 34 kDa and a PDI of 1.34. The *in vitro* drug-release studies showed that the Dex release from the conjugate was triggered by low pH. Clinical measurements, endpoint bone mineral density (BMD) test and histology grading from the *in vivo* evaluation all suggest that newly synthesized P-Dex has strong and long-lasting anti-inflammatory and joint protection effects.

Conclusions—A HPMA copolymer-dexamethasone conjugate with a well-defined structure has been synthesized and proved to be an effective anti-arthritis therapy. It may have a unique clinical application in the treatment of rheumatoid arthritis.

Keywords

Macromolecular Therapy; Rheumatoid Arthritis; Dexamethasone; RAFT polymerization; Drug Delivery

Introduction

Rheumatoid arthritis (RA) is a chronic inflammatory disease of unknown etiology and complex multifactorial pathogenesis, affecting approximately 0.8 percent of adults worldwide. RA is

5 To whom correspondence should be addressed. (e-mail: dwang@unmc.edu).
4These authors contributed equally to this work.

characterized by destructive inflammation of joints, with the eventual deterioration of the articular bone and cartilage (1,2). Improved understanding of the pathophysiology of RA has led to several effective therapeutic strategies for the treatment of RA, such as nonsteroidal anti-inflammatory drugs (NSAIDs), glucocorticoids (GCs), and disease-modifying anti-rheumatic drugs (DMARDs) (3,4). These drugs are relatively safe and effective in the short-to-intermediate–term treatment of RA. However, long-term use may result in various, sometimes severe, side effects (5-7). While the management of RA continues to evolve with many new drugs (e.g. gene therapy) under investigation (3,4,8,9), most of them do not have arthrotropicity. Generally, this lack of tissue specificity combined with the ubiquitous distribution of the molecular targets may explain the significant systemic and extra-articular adverse events often associated with antirheumatic drugs (10,11).

The discovery of novel joint-specific molecular targets may address this problem head-on. From a practical angle, however, drug delivery offers a simple solution by incorporating the arthrotropism to available antirheumatic drugs (12,13). These newly developed strategies capitalize on two unique pathophysiological conditions of RA joints: the enhanced vascular permeability to macromolecules, and the relatively acidic local environment. RA is characterized by synovial proliferation with chronic inflammatory cell infiltration and neovascularization (14). These pathologic neoangiogenic vessels are similar to that in tumors and tend to exhibit disordered architecture and have enhanced permeability to macromolecules compared with normal vessels (15,16). The local inflammatory reaction in and around RA joint tissues also promotes an acidic environment known as acidosis. This is partially due to the low levels of oxygen in the synovial fluid, which appears to induce a shift towards anaerobic glycolysis and lactate formation (17,18). The pH values of synovial fluid had been reported as low as 6.0 (19). Much lower pH values (4.4-5.6) in the synovial tissue have also been reported (20-22).

The leaky vasculature of RA joint has been successfully exploited in targeted glucocorticoid therapy. Long-circulating liposomes loaded with GC could remain in the circulation with a long half-life and extravasate selectively into the inflamed joints with high concentrations. These formulations may increase the therapeutic index of GCs and enable their use as both short-term treatment and prolonged therapy for RA (23-26).

Similar to the liposome approach, we found that synthetic water-soluble polymers, such as *N*-(2-hydroxypropyl)methacrylamide (HPMA) copolymers have strong arthrotopicity when administered to adjuvant-induced arthritis rats (AIA) (13). Based upon this finding, our group developed a HPMA copolymer-dexamethasone conjugate (P-Dex) with a pH-sensitive drug activation mechanism that would further enhance the RA joint specificity of the delivery system (27). Results from an initial *in vivo* evaluation suggested that the conjugate offers superior and longer-lasting anti-inflammatory effects when compared with free Dex. Greater bone and cartilage preservation is also observed with the P-Dex treatment. However, the inconsistency of drug-loading from batch to batch is a challenge that may hamper its translation into clinical application. This problem is largely due to the synthetic strategy that has been employed. As the modification of the HPMA copolymer precursor proceeds, unreacted pendent functionalities will be left with each polymer analogous reaction step. Regardless, the final Dex loading is hard to control.

To address this issue, a new pH-sensitive Dex-containing monomer has been designed, synthesized and reported in this manuscript. Direct copolymerization of this monomer with HPMA allows easy control of Dex loading in the conjugate. No unreacted pendent functionalities will exist in the drug conjugate. Reversible addition-fragmentation transfer (RAFT) polymerization was used to copolymerize the novel Dex-containing monomer with HPMA. This method provides better control of the polydispersity of the polymer drug

conjugate. The therapeutic efficacy of this novel HPMA copolymer-Dex conjugate was evaluated using AIA rats.

Materials and Methods

Materials

S,*S*′-Bis(α,α′-dimethyl-α″-acetic acid)-trithiocarbonate (28), *N*,*N*-dioctadecyl-*N*′,*N*′-bis(2-hydroxyethyl)-1,3-propanediamine (LA) (29), HPMA (30), *N*-methacryloylaminopropyl fluorescein thiourea (MA-FITC) (31) and *N*-methacryloylglycylglycine (MA-Gly-Gly-OH) (32) were prepared as described previously. Sephadex LH-20 resin was obtained from GE Healthcare (Piscataway, NJ, USA). *Mycobacterium tuberculosis* H37Ra (heat-killed, desiccated) was obtained from VWR International (West Chester, PA, USA). Paraffin oil (low viscosity, Bayol F) was obtained from Crescent Chemical Company, Inc. (Islandia, NY, USA). Dexamethasone (Dex) was purchased from Hawkins, Inc. (Minneapolis, MN, USA). All solvents and other reagents if not specified were purchased from Fisher Scientific (Pittsburgh, PA, USA) and used without further purification.

Instruments

^{1}H and ^{13}C NMR spectra were recorded on a 500 MHz NMR spectrometer (Varian, Palo Alto, CA, USA). The mass spectrum analyses were performed with a LC/MS/MS system composed of an ACQUITY Ultra Performance LC (UPLC) system (Waters, Milford, MA, USA) and a mass spectrometer of Sciex 4000 Q TRAP with an ESI source (Applied Biosystems, Toronto, Canada). All chromatographic separations were performed with a C_{18} column (Waters, 100×2.1 mm, 1.7 μm). The mobile phase consisted of 5% ACN in MeOH (mobile phase A) and 7.5 mM ammonium acetate, pH 6 (mobile phase B). The LC flow consisted of 45% mobile phase A and 55% mobile phase B at a total flow rate of 0.3 mL/min. The weight average molecular weight (M_w) and number average molecular weight (M_n) of copolymers were determined by size exclusion chromatography (SEC) using the ÄKTA FPLC system (GE HealthCare) equipped with UV and RI (KNAUER, Berlin, Germany) detectors. SEC measurements were performed on Superdex 200 column (HR 10/30) with phosphate-buffered saline (pH = 7.3) as the eluent. HPMA homopolymer (PHPMA) samples with narrow polydispersity were used as calibration standards. HPLC analyses were performed on an Agilent 1100 HPLC system (Agilent Technologies, Inc., Santa Clara, CA, USA) with a reverse phase C_{18} column (Agilent, 4.6×250 mm, 5 μm). Bone mineral density (BMD) was measured with a pDEXA® Sabre™ X-ray bone densitometer (Norland Medical System, Inc., Fort Atkinson, WI, USA)

Synthesis of *N*-methacryloylglycylglycyl hydrazide (MA-Gly-Gly-NHNH$_2$, Scheme 1)

N-Methacryloylglycylglycine (MA-Gly-Gly-OH, 0.8 g, 4 mmol) was suspended in ethanol (15 mL) at 0°C. Small amount of inhibitor (tert-octyl pyrocatechine) was added into the solution to prevent polymerization. *N*,*N*′-Dicyclohexylcarbodiimide (DCC, 0.9 g, 4.4 mmol) in ethanol (5 mL) was added into the reaction solution. The reaction mixture was stirred for 2 h at 0°C and 2 h at room temperature and then filtered to remove dicyclohexylurea (DCU) at 0°C. Hydrazine hydrate (0.4 mL) in ethanol (5 mL) was then added into the filtrate and the solution was stirred for 4 h at room temperature. When crystalline material started to precipitate, hexane (25 mL) was added and the final product was filtered and washed with ethanol-hexane (1:1, v/v). Yield: 60 %.

^{1}H NMR (d_6-DMSO) δ (ppm): 8.94 (s, 1 H), 8.15 (t, J = 5.9 Hz, 1 H), 8.07 (t, J = 5.9 Hz, 1 H), 5.74 (s, 1 H), 5.38, (s, 1 H), 4.20 (s, 2 H), 3.76 (d, J = 5.9 Hz, 2 H), 3.67 (d, J = 5.9 Hz, 2 H), 1.88 (s, 3 H); ^{13}C NMR (d_6-DMSO) δ (ppm): 169.5, 168.3, 167.9, 139.6, 120.0, 42.7, 41.1, 18.8.

Synthesis of pH-sensitive, Dex-containing monomer (MA-Gly-Gly-NHN=Dex, Scheme 1)

N-Methacryloylglycylglycyl hydrazide (200 mg, 1 mmol) and Dex (390 mg, 1 mmol) were dissolved in methanol (9 mL). Acetic acid (0.5 mL) was added to the reaction solution as a catalyst. The solution was purged with Argon and stirred for 3 days at room temperature in a sealed ampule. After evaporation of the reaction solvent, the product was purified by flash column chromatography (chloroform/ethanol = 8:1, v/v). Yield: 30 %.

^{1}H NMR (d_6-DMSO) δ (ppm): 10.84 (s, 0.5 H), 10.49 (s, 0.5 H), 8.19 (t, J = 6.3 Hz, 1 H), 8.10 (t, J = 6.3 Hz, 0.5 H), 7.88 (t, J = 6.3 Hz, 0.5 H), 6.78 (s, 0.5 H), 6.68 (s, 0.5 H), 6.45 (dd, J_1 = 15.6 Hz, J_2 = 10.2 Hz, 1 H), 6.24 (dd, J_1 = 24.9 Hz, J_2 = 10.2 Hz, 1 H), 5.73 (s, 1 H), 5.37 (s, 1 H), 5.12 (br, 1 H), 4.92 (s, 1 H), 4.66 (br, 1 H), 4.48 (dd, J_1 = 19.0 Hz, J_2 = 5.4 Hz, 1 H), 4.09 (m, 3 H), 3.86 (m, 1 H), 3.77 (m, 2 H), 2.93 (m, 1 H), 2.61 (m, 1 H), 2.19 (m, 4 H), 1.87 (s, 3 H), 1.72 (m, 1 H), 1.60 (q, 1 H, 10.6 Hz), 1.41 (s, 3 H), 1.20 (m, 3 H), 0.84 (s, 3 H), 0.77 (d, 3 H, J = 6.8 Hz); ^{13}C NMR (d_6-DMSO) δ (ppm): 211.4, 170.6, 169.5 (d, *syn* and *anti* conformation), 167.8 (d, *syn* and *anti* conformation), 165.6, 157.2 (d, *syn* and *anti* conformation), 143.1, 139.7 (d, *syn* and *anti* conformation), 139.0, 126.5, 119.9 (d, *syn* and *anti* conformation), 100.8 (d, J_{CF} = 173 Hz), 90.3, 70.1 (d, J_{CF} = 37 Hz), 66.5, 47.6, 47.3 (d, J_{CF} = 22 Hz), 43.6, 42.5 (d, *syn* and *anti* conformation), 40.6 (d, *syn* and *anti* conformation), 36.0, 35.1, 34.0 (d, J_{CF} = 20 Hz), 32.2, 31.0, 27.5, 24.4 (d, J_{CF} = 6 Hz), 18.7, 16.8, 15.5. The syn/anti diastereomers were chromatographically separated using LC/MS/MS with chromatography conditions stated in the Instruments section. Mass Spectra (negative ion ESI) for both isomers showed the molecular ion $[M-H]^-$ at 587.3, which confirms their monoisotopic mass of 588.3.

Synthesis of HPMA copolymer-Dex conjugate (P-Dex) via RAFT copolymerization (Scheme 2)

HPMA (444 mg, 3.1 mmol) and MA-Gly-Gly-NHN=Dex (128 mg, 0.22 mmol) were dissolved in methanol/DMF (6:1, v/v), with 2,2′-azobisisobutyronitrile (AIBN, 2.7 mg, 0.016 mmol) as initiator and S,S′-bis(α, α′-dimethyl-α″-acetic acid)-trithiocarbonate as RAFT agent. Trace amount of MA-FITC was also added into the copolymerization solution to afford the final product a fluorescent tag for easy detection in purification. The solution was purged with Argon and polymerized at 50°C for 2 days. The resulting polymer was first purified on a LH-20 column to remove the unreacted low molecular weight compounds, and then dialyzed. The molecular weight cutoff of the dialysis tubing is 25 kDa of globular protein. The polymer solution was lyophilized to obtain the final P-Dex. Yield: 250 mg.

To quantify Dex loading in P-Dex, it was hydrolyzed in 0.1 N HCl (1 mg/mL) overnight. The resulting solution was neutralized and analyzed with HPLC. Mobile phase, acetonitrile/water = 2/3; Detection, UV 240 nm; Flow rate, 1 mL/min; Injection volume: 10 μL. The analyses were performed in triplicate. The mean value and standard deviation were obtained with Microsoft Excel.

In vitro Dex release from P-Dex

P-Dex (2 mg/mL) was dissolved in acetate buffer (0.01 M with 0.15 M NaCl, pH 5.0) or phosphate buffer (0.01 M with 0.15 M NaCl, pH 7.4) and incubated at 37°C. At selected time intervals, the P-Dex solution (0.3 mL) was withdrawn and neutralized for HPLC analysis. The analysis of each sample was performed in triplicate. The mean value and standard deviation were obtained with Microsoft Excel.

Treatment of AIA rats with P-Dex

Male Lewis rats (175 to 200 g) were obtained from Charles River Laboratories, Inc. (Wilmington, MA, USA) and allowed to acclimate for at least 1 week. To induce arthritis, *Mycobacterium tuberculosis* H37Ra (1 mg) and LA (5 mg) were mixed in paraffin oil (100 μL), sonicated and injected subcutaneously into the base of the tail (33). The progression of the joint inflammation was monitored daily. Special care was given to the rats as the inflammation developed to ensure access to water and food. All animal experiments were performed according to a protocol approved by the University of Nebraska Medical Center Institutional Animal Care and Use Committee and adhered to *Principles of Laboratory Animal Care* (National Institutes of Health publication 85–23, revised in 1985).

Rats with established arthritis were selected and randomly assigned into three groups, P-Dex, free Dex, and saline, with 6-7 AIA rats per group. Six healthy, untreated rats were also included as a control group. On the 14^{th} day post arthritis induction, P-Dex (100 mg/kg, $[Dex]_{P\text{-}Dex}$ = 100 mg/g of P-Dex) was given intravenously to one group of AIA rats. An equivalent dose of free Dex (10 mg/kg of free Dex in the form of water-soluble dexamethasone sodium phosphate) was divided into four aliquots (2.5 mg/kg of free Dex) and was administered (i.p.) to the second group of AIA rats on days 14, 15, 16, and 17. Saline was given similarly to the third group of AIA rats. The clinical measurements of ankle joints were performed daily. On day 24, all animals were euthanized. The hind limbs were dissected at the knee joint. The BMDs (right leg) of the region from distal tibia to the phalanges of the foot were measured by peripheral dual energy x-ray absorptiometry (pDEXA).

Clinical measurements

The clinical parameters measured during the treatment included articular index (AI) score and ankle diameter. AI scores were taken for each hind paw by the same observer from day 8 to 24 and the sum of the score from each animal was recorded. The AI scoring for arthritis was performed using a 0-4 scale, where 0 = no signs of swelling or erythema, 1 = slight swelling and/or erythema, 2 = low-to-moderate edema and signs involving the tarsals (proximal part of the hind paw), 3 = pronounced edema with limited use of the joint and signs extending to the metatarsals, 4 = excessive edema with joint rigidity and severe signs involving the entire hind paw. Clipper measurements of ankle diameter (medial to lateral) were taken every day from day 8 to 24 using a digital caliper (World Prescision Instruments, Inc. Saraspta, FL, USA).

Histological analysis

The hind limbs were isolated and fixed with buffered formalin (10 %) for 3 days and decalcified with 12.5% (v/v) HCl for at least 2 more days. The decalcification solution was replaced with fresh solution every 24 hours. When decalcification was complete, the ankle joint was transected along the longitudinal plane to give approximately equal halves. Each half joint was then embedded in paraffin. Sections (5 μm thickness) from each ankle joint were cut approximately 200 μm apart and stained using a standard hematoxylin and eosin (H & E) staining method. The joints were histologically scored according to a grading system modified from the literature (34). The histological changes of joints were graded on the following parameters: synovial cell lining hyperplasia (0-2); villous hyperplasia (0-3); mononuclear cell infiltration (0-3); polymorphnuclear leukocytes infiltration in periarticular soft tissue (0-3); cellular infiltration and bone erosion at the distal tibia (0-2) and cellular infiltration of cartilage (0-1) (Table 1). The histology score was then recorded for each ankle joint and summarized for each animal by two independent examiners (JT and KF), who were blinded to the treatment the animal received.

Statistical methods

One-way analysis of variance (ANOVA) was performed followed by a post hoc test (Tukey-Kramer) for multiple comparisons using Instant Biostatistics (Version 3.0, GraphPad Software, La Jolla, CA, USA). A value of $P < 0.05$ was considered statistically significant.

Results

Syntheses of MA-Gly-Gly-NHN=Dex and P-Dex

As the first step in synthesis of MA-Gly-Gly-NHN=Dex, MA-Gly-Gly-$NHNH_2$ must be obtained. MA-Gly-Gly-OH was reacted with ethanol to form an ethyl ester. It was then hydrazinolyzed to obtain MA-Gly-Gly-$NHNH_2$ with about 60 % of yield. This route was proved to be very simple with easy purification workup. To obtain the final hydrazone-containing Dex monomer, Dex was initially reacted with MA-Gly-Gly-$NHNH_2$ in DMF using acetic acid or HCl as a catalyst. The reaction was not successful. Switching solvent to methanol greatly improved the efficency of reaction. After flash column chromatography, the final product was obtained with 30 % of yield. The structures of MA-Gly-Gly-NHN=Dex (syn/anti diastereomers, ratio ≈ 1:1, Scheme 3) were first revealed by ^{1}H and ^{13}C NMR spectra. They were then confirmed with LC/MS/MS analysis. Two peaks were found in the LC spectrum. They both yielded a strong molecular ion $[M-H]^-$ with a mass of 587.3 in the negative ionization mode, which agrees with the monoisotopic mass of 588.3 for MA-Gly-Gly-NHN=Dex. Using MS/MS analysis, the fragmentation patterns of the diastereomers were studied. The most abundant fragments were at 557.1 due to the loss of a hydroxymethyl group and at 180.0 due to the breakage of the bond between MA-Gly-Gly-NH and N=Dex with additional loss of a H_2O molecule. No attempt was made to separate the diastereomers. Using AIBN as the initiator and S,S′-bis(α, α′-dimethyl-α″-acetic acid)-trithiocarbonate as the RAFT agent, MA-Gly-Gly-NHN=Dex was copolymerized with HPMA. After purification with LH-20 column and dialysis, the FPLC analysis results showed that the weight average molecular weight (M_w) of P-Dex is 34 kDa with a polydispersity index (PDI) of 1.34, which is narrower than a regular free radical polymerization of HPMA (PDI = 1.5-1.6). The Dex content in the P-Dex was determined as 100 mg/g of P-Dex. Conversion of MA-Gly-Gly-NHN=Dex in the copolymerization is about 50 %. When the feed-in ratio of Dex monomer changed, the convention ratio was kept at about 50 %. The HPLC analysis showed that 99.2 % of Dex content was covalently conjugated to the polymer. The 0.8 % free Dex detected in the purified P-Dex may come from the dialysis step. This conjugate was used for *in vitro* Dex release study and *in vivo* treatment study of the AIA rats.

In vitro Dex release from P-Dex

The *in vitro* Dex release was studied by incubating P-Dex in pH 5.0 and pH 7.4 at 37°C (Figure 1). Under neutral condition, there is almost no Dex release from P-Dex; while at pH 5.0, Dex was gradually released from the conjugate. During the course of the experiment (14 days), P-Dex demonstrated a zero-order release at pH 5.0. The release rate of Dex from P-Dex is about 1% of the loaded drug per day.

Clinical evaluations of AIA rats treated with P-Dex, free Dex and saline

The therapeutic effect of P-Dex was evaluated on AIA rats in comparison with free Dex, saline and healthy controls. On day 8 to 9 post arthritis induction, the disease started with the onset of mild swelling and increased ankle diameter (Figures 2 & 3). The ankle joint inflammation continues to worsen, and by day 13 to 14, the swelling started to plateau. All treatments were initiated on day 14. The response to treatments by both free Dex and P-Dex were immediate and very significant. As shown in Figures 2 & 3, ankle size and AI scores for these two groups were greatly reduced on day 15. The animals were more mobile and active. Upon cessation of

the free Dex treatment on day 18, inflammatory flare was observed, with a rapid decrease in mobility. By the end of the study on day 24, the animals that had been treated with free Dex were indistinguishable from those in the saline group in terms of ankle diameter and AI scores. Contrary to the free Dex treatment, single P-Dex treatment strongly suppressed the ankle joint inflammation during the entire course of the treatment. It was maintained at the end of the study (euthanasia on day 24).

BMD assessment

The measurement of BMD from distal tibia to the phalanges of the foot of all animals was performed at the end of the study (Figure 4). One-way analysis of variance (ANOVA) produced a P value of less than 0.01, considered significant. The saline group was found to have the lowest mean BMD values of 0.156, followed by free Dex group (BMD = 0.165) and P-Dex group (BMD = 0.175). The healthy control group showed the highest mean BMD value of 0.178 among the four groups. From the pDEXA images, we found that the major bone destruction of arthritic joints happened at distal tibia, with minor BMD reduction at carpal and metacarpal bones.

Histological evaluation of ankle joints

As shown in Figure 5, the saline group was found with the highest histological score of 12.8, indicating severe inflammation and joint destruction. It was followed by free Dex group with a slightly lower score of 9.3. P-Dex treatment, on the other hand, shows the lowest histology score of 1.3, which is very close to the score of 0 of the healthy reference group. One-way analysis of variance (ANOVA) produced a P value of less than 0.0001, considered significant. Figure 6 composes of photomicrographs of representative H & E sections from each group. All animals from the saline treated group showed the highest scores in each parameter of histological grading. Severe bone destruction of the distal tibia and cartilage erosion of the joint are present. In the free Dex treatment group, synovial cell lining and villous hyperplasia are moderate in most of the cases. Polymorphonuclear leukocyte infiltration into periarticular soft tissue fluctuated between mild and moderate levels. Bone and cartilage destruction was present in all cases. Compared to these two groups of animals, P-Dex treatment demonstrates the best anti-inflammatory effect with profound bone and cartilage protection. Polymorphonuclear leukocyte infiltration into periarticular soft tissue, cellular infiltration of cartilage, cellular infiltration and bone destruction at the distal tibia are absent in most cases, which is similar to the healthy control group. Thin rim of synovial cell lining with mildly increased cellular activity was observed, suggesting the presence of minor synovitis.

Discussion

Development of drug delivery strategies for the improved treatment of rheumatoid arthritis is an emerging research area. Instead of searching for new molecular targets, it seeks to improve the therapeutic efficacy and safety profile of current available therapies. Due to the angiogenesis and leaky vasculature associated with inflammatory joints, macromolecules and colloidal vesicles can extravasate preferentially at arthritic joints (12,13). Based on this pathological arthrotropism, long-circulating liposome have been proposed as a vehicle to deliver glucocorticoids to arthritic joints for the treatment of RA (23-26). Similarly, our group has found that synthetic water-soluble polymers such as HPMA copolymers could also passively accumulate in arthritic joints. The single administration of a pH-sensitive HPMA copolymer-Dex conjugate was able to suppress joint inflammation for 10 days (27). Between these two delivery systems, liposome formulation is certainly easier to prepare. The pH-sensitive HPMA copolymer-Dex conjugate, on the other hand, has much better control in drug activation and release because the drug is covalently conjugated to the polymer carrier via

hydrazone bond that can be activated at the arthritic joints via local acidic environment (acidosis and/or lysosome).

Polymer analogous reaction was used in the initial synthesis of HPMA copolymer-Dex conjugates (27). While it was proven to be a very simple strategy, the inherited inconsistency of drug loading from batch to batch and residual pendent functionalities (-COOH and $-CONHNH_2$) of the method may impede the translation of this promising therapy into clinical applications. To resolve these problems, a new synthetic route was designed. First, a pH-sensitive Dex-containing monomer, MA-Gly-Gly-NHN=Dex was synthesized (Scheme 1). It was copolymerized with HPMA (Scheme 2). By doing this, it was possible to precisely control the drug-loading ratio and completely avoid the residual pendent functionalities.

The synthesis of MA-Gly-Gly-$NHNH_2$ was done by hydrazinolysis of the ethyl ester of MA-Gly-Gly-OH at room temperature with simple purification workup. However, the synthesis of MA-Gly-Gly-NHN=Dex has proven to be very difficult because both the reactant and the product can polymerize prematurely. To dissolve both Dex and MA-Gly-Gly-$NHNH_2$ for the reaction, DMF was first selected as the solvent with acetic acid as catalyst. After a 3-day reaction at room temperature, no product was formed even at an 1:1 molar ratio of catalyst to reactant. When the reaction temperature was elevated to accelarate the reaction, polymerization occurred. When HCl was tested as the catalyst, several byproducts were formed, which cause the purification to be extremely difficult. After several trials, methanol was selected as the best reaction solvent. MA-Gly-Gly-NHN=Dex was obtained as the main product at room temperature with acetic acid as the catalyst. The yield was 30 %, which needs further improvement. This is partially due to fact that a rather mild reaction condition was selected to avoid premature polymerization during the synthesis. From NMR spectra of the product, C-3 carbonyl (not C-18) was found to react with MA-Gly-Gly-$NHNH_2$ to form a hydrazone bond. Flash column chromatography was used to separate the product from the reactants (> 50 % of Dex was not reacted) and small amount of side products. As we did not analyze the side products, the potential of reaction at C-18 carbonyl can not be ruled out. Compounds containing hydrazone functional groups are known to often exist as diastereomers (35,36). The presence of an additional nitrogen atom decreases the C=N double bond character of the π-system and facilitates isomerization (37). Both the NMR and LC/MS/MS results confirmed the existence of syn/anti diastereomers of MA-Gly-Gly-NHN=Dex (Scheme 3) with a molar ratio close to 1:1. Because the cleavage of the hydrazone bonds in both diastereomers would produce Dex, they were not futher separated but used directly in the next step to synthesize HPMA copolymer-Dex conjugate.

HPMA copolymers are biocompatible, nonimmunogenic and nontoxic. It is the most extensively studied drug carrier, with more than half of all polymeric drug conjugates in clinical evaluations based on this polymer (38-40). HPMA copolymers are generally prepared by free radical copolymerization and have a regular PDI of 1.5-1.6. Due to the impact this wide polydispersity may have on pharmacokinetics, safety and efficacy of polymer therapeutics, a narrower PDI is very desirable. Recently, reversible addition-fragmentation transfer (RAFT) polymerization has emerged as an alternative controlled radical polymerization technique because it can lead to the synthesis of many well-defined polymers with predictable molecular weights, and it works very well with most acrylic derivatives including acrylic acid (41,42). Several carboxyl-terminated trithiocarbonates have been developed as novel RAFT agents (28) and used in RAFT polymerization of different monomers, including HPMA (43). These trithiocarbonates have extremely high chain-transfer efficiency and can yield polymers with narrow polydispersity and predictable molecular weights. In this study, RAFT polymerization was used to copolymerize MA-Gly-Gly-NHN=Dex and HPMA with S,S′-bis(α,α′-dimethyl-α″-acetic acid)-trithiocarbonate as the RAFT agent. After extensive optimization of the polymerization conditions, the M_w of P-Dex obtained for our animal studies was 34 kDa with

a PDI of 1.34, which is significantly lower than traditional free radical copolymerization of HPMA. The incorporation efficacy of MA-Gly-Gly-NHN=Dex into P-Dex is about 50 %. This conversion ratio remained constant when the feed-in ratio of the Dex monomer was changed. Thus, the drug loading in the HPMA conjugate can be precisely controlled and repeated simply by maintaining the monomer feed-in ratio. Further improvement is still needed to increase the Dex monomer conversion ratio while retaining the narrow PDI of the copolymer conjugate.

For the newly synthesized P-Dex, it was necessary to demonstrate the same pH-sensitivity as the HPMA copolymer-Dex conjugate we synthesized previously with polymer analogous reaction (27). This feature is critical for the delivery system, as it will allow for the activation and release of Dex in the arthritic joints, where joint acidosis and the low pH of lysosomes will act as the local activation triggers. As can be seen in Figure 1, the release of Dex from the conjugate was indeed pH-sensitive. At pH 5.0, the Dex release from the conjugate is of zero order. This is similar to our previous results from HPMA copolymer-Dex conjugate synthesized with polymer analogous reaction (27). The release rate is around 1 % per day. Under neutral condition, the release of Dex from P-Dex is extremely low, which ensures that the drug conjugate would not be activated prematurely in the circulation. While this *in vitro* experiment proved the pH-sensitivity of the newly synthesized P-Dex, we suspect that the release rate of Dex from the conjugate in the arthritic joint may be faster, as suggested by the data of the *in vivo* experiment.

To test the therapeutic efficacy of P-Dex *in vivo*, P-Dex was administer to AIA rats on days 14^{th} post arthritis induction as a single bolus i.v. administration. Equivalent dose of free Dex was made into 4 aliquots and administered i.p. on days 14-17. Saline group and healthy group were used as two control groups. As can be seen in Figures 2 and 3, both AI score and the ankle diameter showed dramatic decreases after the initiation of the P-Dex and free Dex treatments, which can be attributed to the well-known potency and fast action of GCs. This result indirectly suggests that the activation of P-Dex is immediate (and probably faster than the *in vitro* release), due to the acidic environment in arthritic joints. The activation may also happen post endocytosis in the lysosomes of macrophage-like synoviocytes. The two treatment groups started to differentiate right after the last dose of free Dex. Arthritis flare happened immediately in the free Dex group, while the P-Dex group continued the healing process until the end of the study. At the end point, the AI score and ankle diameter of the free Dex group is at the same level as the saline group. The P-Dex group, on the other hand, is very similar to the healthy group. Compared to free Dex, the anti-inflammatory effect of P-Dex is clearly much longer. The retention of the polymeric drug conjugate in arthritic joints (13) and the gradual activation (low pH mediated) of Dex may together contribute to the observed superior anti-inflammatory effect of P-Dex.

Bone and cartilage destruction are often associated with RA joints. To investigate if P-Dex would preserve bone, we performed endpoint BMD evaluation of the arthritic joints from different treatment groups. From Figure 4, it is obvious that both free Dex and P-Dex treatments provide bone preservation when compared to the saline group. This may be attributed to their immediate suppression of joint inflammation after administration. This result clearly echoes the disease modifying effects of low dose glucocorticoids observed in human clinical trials (44). The mean BMD of the P-Dex treated group is higher than the group treated with free Dex group, suggesting that the prolonged suppression of inflammation by P-Dex offers better protection to the bone.

Synovial hypertrophy and villous hyperplasia is the major histopathological characteristics in the early stages of RA. The ongoing synovitis, especially the invasive pannus tissue leads to the destruction of the joint cartilage and bone if effective treatment is not initiated. To gain a better understanding of different treatments on joint inflammation at the microscopic level, the

isolated joints were decalcified, sectioned and evaluated histologically (Figures 5 & 6). The histological grading showed dramatic difference among the treatment groups. While the free Dex group seems to offer some clinical improvement, it is not comparable to the strong and long lasting anti-inflammatory and joint protective benefits provided by the P-Dex treatment. We do not know if the very mild synovial cell lining and villous hyperplasia observed in P-Dex group is the result of an ongoing healing process or the prelude of the arthritic flare.

From the data obtained, it is obvious that the P-Dex has a superior and long lasting therapeutic effect for the treatment of RA when compared to free Dex. It was also confirmed that the therapeutic efficacy of the newly synthesized P-Dex was comparable to the HPMA copolymer-Dex conjugate synthesized previously using polymer analogous reaction (27). As a unique advantage, the new P-Dex has a well-define chemical structure, which will facilitate its translation into clinical applications.

While further development of the new P-Dex is very promising, many questions still remain. The huge potential of P-Dex in reducing the systemic side effects of GCs have not been fully investigated due to the lack of a proper animal model; The mechanism of long lasting therapeutic benefits of P-Dex needs to be elucidated; The study was ended 10 days post treatment initiation due to the concern of the welfare of the saline group. Therefore, it is still not clear how long the therapeutic effect of P-Dex will last beyond this 10 days period. This question is clinically relevant because a once-a-month infusion will certainly have a better patients' compliance than a once-a-week infusion.

Conclusion

A novel pH-sensitive Dex-containing monomer (MA-Gly-Gly-NHN=Dex) was designed, synthesized and copolymerized with HPMA using RAFT copolymerization. The resulting P-Dex has a well-defined structure, controllable molecular weight and low PDI. The Dex loading in the conjugate can be simply controlled by adjusting monomer feed-in ratio. The *in vivo* evaluation showed that the newly synthesized P-Dex offers superior and longer-lasting anti-inflammatory effects when compared to free Dex. This finding confirms the previous finding with HPMA copolymer-dexamethasone conjugate synthesized via polymer analogous reactions. The development of this well-defined polymer-drug conjugate is one step further to its clinical application. Additional research efforts are warranted to elucidate its full therapeutic potential.

Acknowledgements

This work was supported in part by NIH grants AR053325 (DW) and AA10435 (GMT), the College of Pharmacy, University of Nebraska Medical Center and the UNeMed Corporation.

References

1. Lawrence RC, Helmick CG, Arnett FC, Deyo RA, Felson DT, Giannini EH, Heyes SP, Hirsh K, Hochberg MC, Hunder GG, Liang MH, Pillemer SR, Steen VV, Wolfe F. Estimates of the prevalence of arthritis and selected musculoskeletal disorders in the United States. Arthritis Rheum 1998;41:778–799. [PubMed: 9588729]
2. Firestein, GS. Etiology and pathogenesis of rheumatoid arthritis. In: Harris, ED., Jr; Budd, RC.; Genovese, MC.; Firestein, GS.; Sargent, JS.; Sledge, CB., editors. Kelley's Textbook of Rheumatology. 7th. Philadelphia: Elsevier Saunders; 2005. p. 996-1042.
3. Smolen JS, Steiner G. Therapeutic strategies for rheumatoid arthritis. Nat Rev Drug Discov 2003;2:473–488. [PubMed: 12776222]
4. O'Dell JR. Therapeutic strategies for rheumatoid arthritis. N Engl J Med 2004;350:2591–2602. [PubMed: 15201416]

5. FitzGerald GA. COX-2 and beyond: Approaches to prostaglandin inhibition in human disease. Nat Rev Drug Discov 2003;2:879–890. [PubMed: 14668809]
6. Baylink DJ. Glucocorticoid-induced osteoporosis. N Engl J Med 1983;309:306–308. [PubMed: 6866054]
7. Borchers AT, Keen CL, Cheema GS, Gershwin ME. The use of methotrexate in rheumatoid arthritis. Semin Arthritis Rheum 2004;34:465–483. [PubMed: 15305245]
8. Olsen NJ, Stein CM. New drugs for rheumatoid arthritis. N Engl J Med 2004;350:2167–2179. [PubMed: 15152062]
9. Traister RS, Hirsch R. Gene therapy for arthritis. Mod Rheumatol 2008;18:2–14. [PubMed: 18176779]
10. Capell H. Longterm maintenance therapy with disease modifying antirheumatic drugs. J Rheumatol Suppl 2002;66:38–43. [PubMed: 12435167]
11. Garrood T, Pitzalis C. Targeting the inflamed synovium: the quest for specificity. Arthritis Rheum 2006;54:1198–1208. [PubMed: 16575845]
12. Boerman OC, Oyen WJ, Storm G, Corvo ML, van Bloois L, van der Meer JW, Corstens FH. Technetium-99m labelled liposomes to image experimental arthritis. Ann Rheum Dis 1997;56:369–373. [PubMed: 9227166]
13. Wang D, Miller SC, Sima M, Parker D, Buswell H, Goodrich KC, Kopečková P, Kopeček J. The arthrotropism of macromolecules in adjuvant-induced arthritis rat model: a preliminary study. Pharm Res 2004;21:1741–1749. [PubMed: 15553217]
14. Koch AE. Angiogenesis as a target in rheumatoid arthritis. Ann Rheum Dis 2003;62:ii60–67. [PubMed: 14532152]
15. Matsumura Y, Maeda H. A new concept for macromolecular therapeutics in cancer chemotherapy: mechanism of tumoritropic accumulation of proteins and the antitumor agent smancs. Cancer Res 1986;46:6387–6392. [PubMed: 2946403]
16. Levick JR. Permeability of rheumatoid and normal human synovium to specific plasma proteins. Arthritis Rheum 1981;24:1550–60. [PubMed: 7326067]
17. Levick JR. Hypoxia and acidosis in chronic inflammatory arthritis; relation to vascular supply and dynamic effusion pressure. J Rheumatol 1990;17:579–582. [PubMed: 2359066]
18. Falchuk KH, Goetzl EJ, Kulka JP. Respiratory gases of synovial fluids. An approach to synovial tissue circulatory-metabolic imbalance in rheumatoid arthritis. Am J Med 1970;49:223–231. [PubMed: 5452943]
19. Goldie I, Nachemson A. Synovial pH in rheumatoid knee-joints. I. The effect of synovectomy. Acta Orthop Scand 1969;40:634–641. [PubMed: 5378127]
20. Andersson SE, Lexmuller K, Johansson A, Ekstrom GM. Tissue and intracellular pH in normal periarticular soft tissue and during different phases of antigen induced arthritis in the rat. J Rheumatol 1999;26:2018–2024. [PubMed: 10493685]
21. Konttinen YT, Mandelin J, Li TF, Salo J, Lassus J, Liljeström M, Hukkanen M, Takagi M, Virtanen I, Santavirta S. Acidic cysteine endoproteinase cathepsin K in the degeneration of the superficial articular hyaline cartilage in osteoarthritis. Arthritis Rheum 2002;46:953–960. [PubMed: 11953972]
22. Konttinen YT, Takagi M, Mandelin J, Lassus J, Salo J, Ainola M, Li TF, Virtanen I, Liljeström M, Sakai H, Kobayashi Y, Sorsa T, Lappalainen R, Demulder A, Santavirta S. Acid attack and cathepsin K in bone resorption around total hip replacement prosthesis. J Bone Miner Res 2001;16:1780–1786. [PubMed: 11585341]
23. Schmidt J, Metselaar JM, Wauben MH, Toyka KV, Storm G, Gold R. Drug targeting by long-circulating liposomal glucocorticosteroids increases therapeutic efficacy in a model of multiple sclerosis. Brain 2003;126:1895–1904. [PubMed: 12805101]
24. Metselaar JM, Wauben MH, Wagenaar-Hilbers JP, Boerman OC, Storm G. Complete remission of experimental arthritis by joint targeting of glucocorticoids with long-circulating liposomes. Arthritis Rheum 2003;48:2059–66. [PubMed: 12847701]
25. Metselaar JM, Van den Berg WB, Holthuysen AE, Wauben MH, Storm G, van Lent PL. Liposomal targeting of glucocorticoids to synovial lining cells strongly increases therapeutic benefit in collagen type II arthritis. Ann Rheum Dis 2004;63:348–353. [PubMed: 15020326]
26. Avnir Y, Ulmansky R, Wasserman V, Even-Chen S, Broyer M, Barenholz Y, Naparstek Y. Amphipathic weak acid glucocorticoid prodrugs remote-loaded into sterically stabilized

nanoliposomes evaluated in arthritic rats and in a Beagle dog: a novel approach to treating autoimmune arthritis. Arthritis Rheum 2008;58:119–129. [PubMed: 18163482]

27. Wang D, Miller SC, Liu XM, Anderson B, Wang XS, Goldring SR. Novel dexamethasone-HPMA copolymer conjugate and its potential application in treatment of rheumatoid arthritis. Arthritis Res Ther 2007;9:R2. [PubMed: 17233911]
28. Lai JT, Filla D, Shea R. Functional polymers from novel carboxyl-terminated trithiocarbonates as highly efficient raft agents. Macromolecules 2002;35:6754–6756.
29. Cronin, TH.; Faubl, H.; Hoffman, WW.; Korst, JJ. Xylenediamines as antiviral agents. US patent 4,034,040. 1977.
30. Kopeček J, Bažilová H. Poly[N-(2-hydroxypropyl)methacrylamide]. 1. Radical polymerization and copolymerization. Eur Polym J 1973;9:7–14.
31. Omelyanenko V, Kopečková P, Gentry C, Kopeček J. Targetable HPMA copolymer-adriamycin conjugates. Recognition, internalization, and subcellular fate. J Control Release 1998;53:25–37. [PubMed: 9741911]
32. Rejmanová P, Labský J, Kopeček J. Aminolyses of monomeric and polymeric p-nitrophenyl esters of methacryloylated amino acids. Makromol Chem 1977;178:2159–2168.
33. Chang YH, Pearson CM, Abe C. Adjuvant polyarthritis. IV. Induction by a synthetic adjuvant: immunologic, histopathologic, and other studies. Arthritis Rheum 1980;23:62–71. [PubMed: 7352945]
34. van Dijke CF, Peterfy CG, Brasch RC, Lang P, Roberts TP, Shames D, Kneeland JB, Lu Y, Mann JS, Kapila SD, Genant HK. MR imaging of the arthritic rabbit knee joint using albumin-(Gd-DTPA) 30 with correlation to histopathology. Magn Reson Imaging 1999;17:237–245. [PubMed: 10215479]
35. Gordon MS, Sojka SA, Krause JG. Carbon-13 NMR of para-substituted hydrazones, phenylhydrazones, oximes, and oxime methyl ethers: substituent effects on the iminyl carbon. J Org Chem 1984;49:97–100.
36. Mirífico MV, Caram JA, Vasini EJ. The true configuration of the benzilosazone isomers. Tetrahedron Lett 2006;47:6919–6922.
37. Dugave C, Demange L. Cis-trans isomerization of organic molecules and biomolecules: implications and applications. Chem Rev 2003;103:2475–2532. [PubMed: 12848578]
38. Duncan R. The dawning era of polymer therapeutics. Nat Rev Drug Discov 2003;2:347–360. [PubMed: 12750738]
39. Kratz F, Abu Ajaj K, Warnecke A. Anticancer carrier-linked prodrugs in clinical trials. Expert Opin Investig Drugs 2007;16:1037–58.
40. Duncan R. Designing polymer conjugates as lysosomotropic nanomedicines. Biochem Soc Trans 2007;35:56–60. [PubMed: 17233601]
41. Chiefari J, Chong YK, Ercole F, Krstina J, Jeffery J, Le TP, Mayadunne RTA, Meijs GF, Moad CL, Moad G, Rizzardo E, Thang SH. Living free-radical polymerization by reversible addition-fragmentation chain transfer: the raft process. Macromolecules 1998;31:5559–5562.
42. Yanjarappa MJ, Gujraty KV, Joshi A, Saraph A, Kane RS. Synthesis of copolymers containing an active ester of methacrylic acid by RAFT: controlled molecular weight scaffolds for biofunctionalization. Biomacromolecules 2006;7:1665–1670. [PubMed: 16677052]
43. Pan HZ, Sima M, Kopečková P, Wu KS, Gao SQ, Liu JH, Wang D, Miller SC, Kopeček J. Biodistribution and Pharmacokinetic Studies of Bone-Targeting *N*-(2-Hydroxypropyl) methacrylamide Copolymer-Alendronate Conjugates. Molecular Pharmaceutics. 2008Epub ahead of print
44. Kirwan JR. The effect of glucocorticoids on joint destruction in rheumatoid arthritis. The Arthritis and Rheumatism Council Low-Dose Glucocorticoid Study Group. N Engl J Med 1995;333:142–146. [PubMed: 7791815]

Abbreviations

AI

articular index

AIA
adjuvant-induced arthritis rats

BMD
bone mineral density

DCC
N,*N*′-dicyclohexylcarbodiimide

DCU
dicyclohexylurea

Dex
dexamethasone

DMARDs
disease-modifying anti-rheumatic drugs

GCs
glucocorticoids

H & E
hematoxylin and eosin

HPMA
N-(2-hydroxypropyl)methacrylamide

LA
N,*N*-dioctadecyl-*N*′,*N*′-bis(2-hydroxyethyl)propanediamine

MA-FITC
N-methacryloylaminopropyl fluorescein thiourea

MA-Gly-Gly-OH
N-methacryloylglycylglycine

MA-Gly-Gly-NHN=Dex
pH-sensitive Dex-containing monomer or *N*-(2-(2-(2-((8*S*,9*R*,10*S*,11*S*,13*S*,14*S*,16*R*,17*R*)-9-fluoro-11,17-dihydroxy-17-(2-hydroxyacetyl)-10,13,16-trimethyl-7,8,11,12,13,15,16,17-octahydro-6*H*-cyclopenta[*a*]phenanthren-3(9*H*,10*H*,14*H*)-ylidene)hydrazinyl)-2-oxoethylamino)-2-oxoethyl) methacrylamide as generated by ChemDraw Ultra 9.0 (CambridgeSoft, Cambridge, MA, USA)

M_n
number average molecular weight

M_w
weight average molecular weight

NSAIDs
nonsteroidal anti-inflammatory drugs

P-Dex
copolymer of MA-Gly-Gly-NHN=Dex and HPMA

pDEXA
peripheral dual energy x-ray absorptiometry

PDI

polydispersity index

SEC

size exclusion chromatography

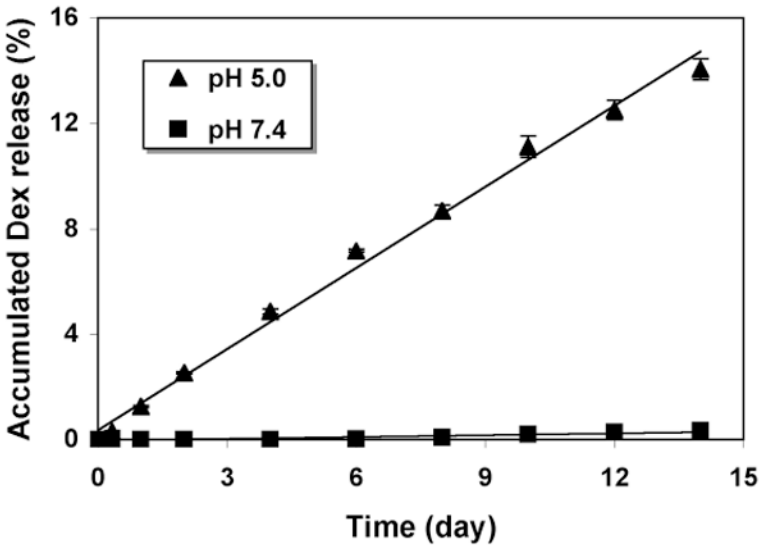

Figure 1.

In vitro Dex release from P-Dex at pH = 5.0 and 7.4. Each sample was measured 3 times. The mean values and standard deviation were calculated with Microsoft Excel. For the linear regression, $R^2 > 0.99$.

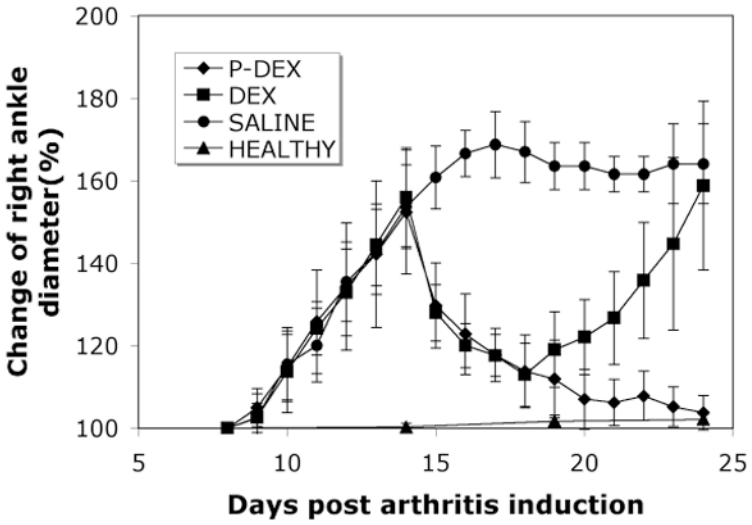

Figure 2.
The change of right ankle joint diameter of the four animal groups (P-Dex, Dex, saline and healthy) during the entire experiment.

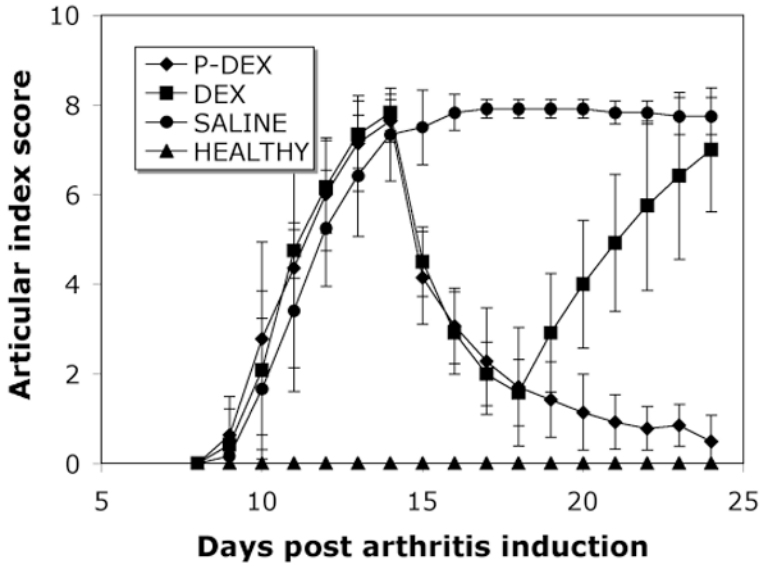

Figure 3.
The change of articular index (AI) score of the four animal groups (P-Dex, Dex, saline and healthy) during the entire experiment.

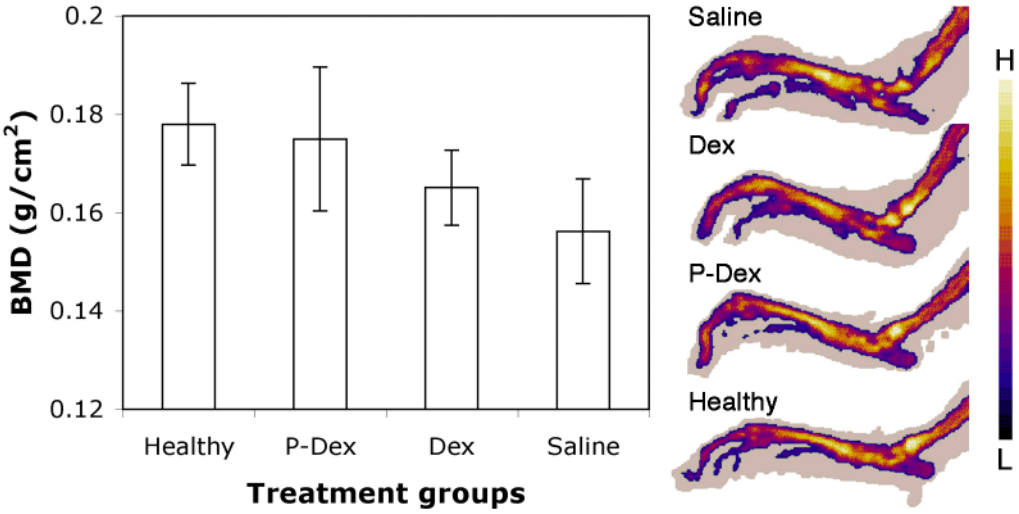

Figure 4.
The endpoint bone mineral density (BMD) and representative pDEXA images of the right ankle joints of the four animal groups (P-Dex, Dex, saline and healthy). One-way ANOVA analysis, $P < 0.01$.

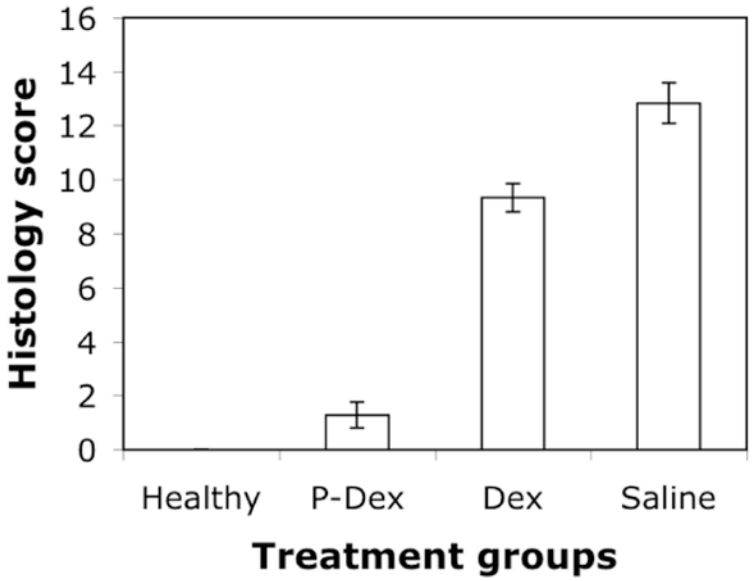

Figure 5.
Histological evaluation of the ankle joints from the four animal groups (P-Dex, Dex, saline and healthy). One-way ANOVA analysis, $P < 0.0001$.

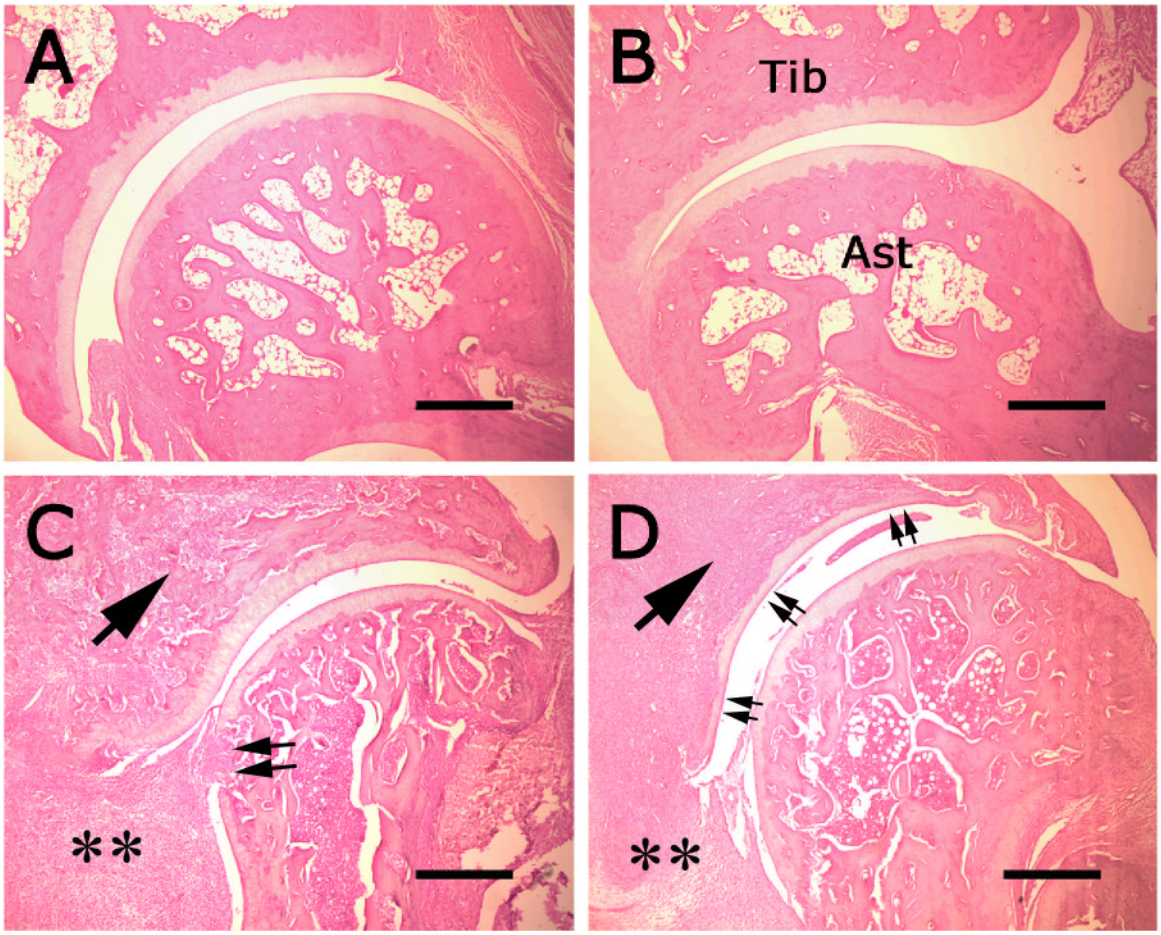

Figure 6.

Representative histology pictures of the ankle joints from the four animal groups. A. P-Dex; B. Healthy; C. Free Dex; D. Saline. Synovial cell lining and villous hyperplasia (**), bone destruction (single arrow) and cartilage damage (double arrow) are clearly evident in free Dex and saline groups. Tib = Tibia, Ast = astrogalus. Bar = 0.5 mm.

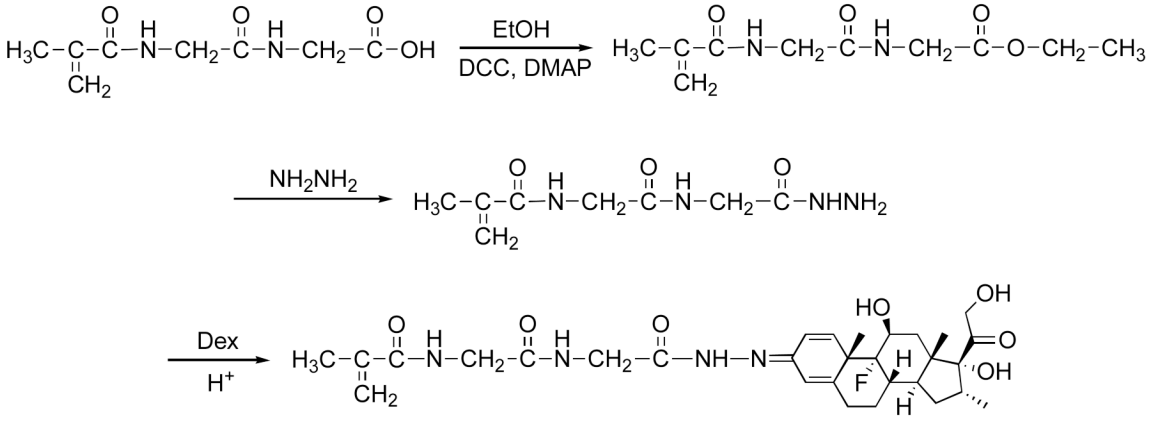

Scheme 1
Synthesis of MA-Gly-Gly-NHN=Dex.

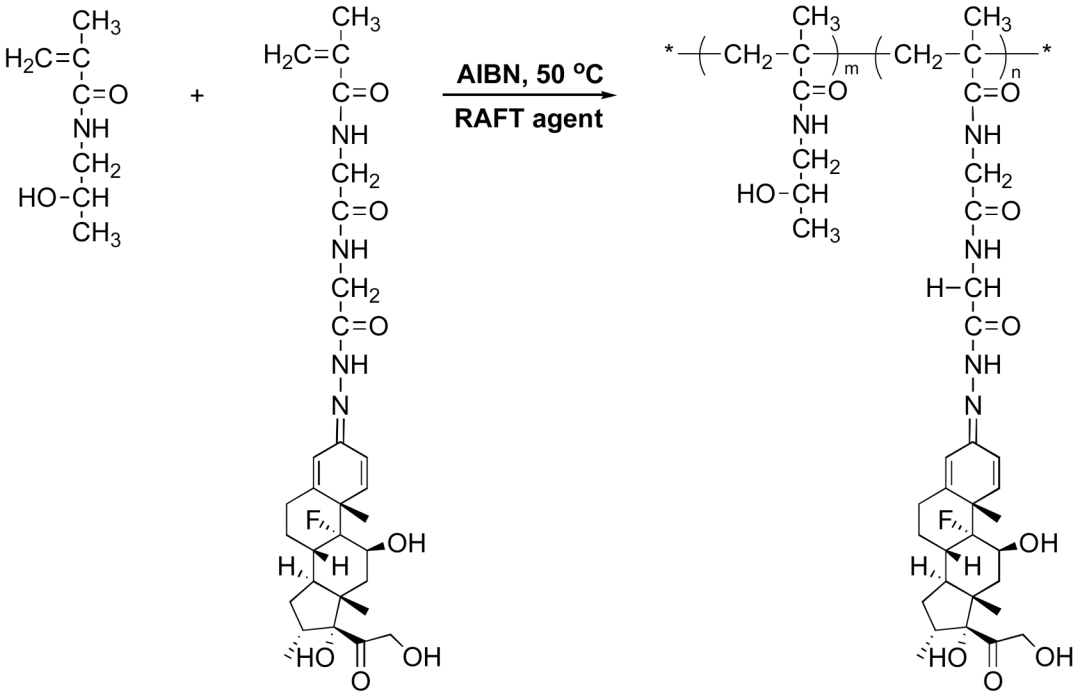

Scheme 2
Synthesis of HPMA copolymer-Dex conjugate (P-Dex) via RAFT copolymerization.

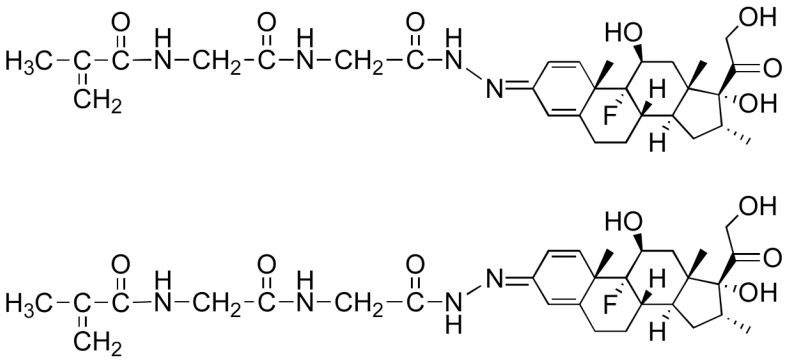

Scheme 3
The structures syn (bottom)/anti (top) diastereomers of MA-Gly-Gly-NHN=Dex.

Table 1

Histological grading system, modified from the method from Ref. 34

Parameters	Grade	Features
Synovial cell lining hyperplasia	0	1 to 3 layers of synoviocytes
	1	4 to 6 layers of synoviocytes
	2	7 or more layers of synoviocytes
Villous hyperplasia	0	Not present
	1	Few, scattered, and short
	2	Moderate and finger-like (form pannus)
	3	More, clustered, and diffuse
Cellular infiltration of mononuclear cells	0	Normal
	1	Mild
	2	Moderate
	3	Severe
Polymorphonuclear leukocyte infiltration into periarticular soft tissue	0	Normal
	1	Mild
	2	Moderate
	3	Severe
Cellular infiltration and bone erosion at the distal tibia	0	Not present
	1	Mild
	2	Moderate
Cellular infiltration of cartilage	0	Not present
	1	Present